Monatshefte für Chemie 133, 799–806 (2002)

Monatshefte für Chemie
Chemical Monthly

A Study of $PbTiO_3$ Crystallization in Pure and Composite Nanopowders Prepared by the Sol-Gel Technique

Marian Čerňanský*, **Přemysl Vaněk, Karel Král,** and **Radmila Krupková**

Academy of Sciences of the Czech Republic, Institute of Physics, CZ-18221 Prague, Czech Republic

Summary. In this investigation the crystallization of $PbTiO_3$ upon annealing of pure nanopowders and $PbTiO_3$–SiO_2 (1:1 v/v) nanocomposite powders prepared by the sol-gel technique was studied. Using X-ray diffraction phase analysis, the start of $PbTiO_3$ crystallization in pure $PbTiO_3$ powders was detected at 400°C. Distinct crystallization of $PbTiO_3$ in $PbTiO_3$–SiO_2 nanocomposites starts at 700°C, whereas SiO_2 remains amorphous. There are indications that an interface interaction between the $PbTiO_3$ and the SiO_2 phase plays an important role in hindering the crystallization of $PbTiO_3$. The particle size (size of coherently scattering regions) was estimated from the broadening of the X-ray diffraction line profiles. The average size of $PbTiO_3$ nanocrystallites increases with temperature and time of annealing, the influence of temperature being more significant than that of the annealing time. Differential scanning calorimetry confirmed the results of the X-ray diffraction with respect to the start of the crystallization. Laser beam scattering and scanning electron microscopy provided the statistical distribution of the grain size and the morphology of the powder grains, showing that each grain of the powders contains several nanocrystallites (coherently scattering regions).

Keywords. Calorimetry; Crystallization; Nanostructures; Sol-gel; X-Ray diffraction.

Introduction

Ferroelectric materials with perovskite crystal structure have several interesting properties which are used in technical applications. Their piezoelectricity is used as a base for electromechanical transducers employed as ultrasonic sensors and generators; detectors of infrared radiation are also based on this property. Ferroelectrics have high dielectric permittivity which is favourable for the fabrication of capacitors of very small size [1]. The transparency of some ceramic ferroelectrics varies under the influence of an electric field, making them promising devices for electro-optic applications. Another important property of these materials is spontaneous polarization which can be reversed by an external electric field [2]. The ability of ferroelectric materials to switch their polarization direction between two

* Corresponding author. E-mail: cernan@fzu.cz

stable polarized states provides the basis for binary-code based nonvolatile ferroelectric random-access memories [3].

The important point is that the physical and technological properties of the perovskite ferroelectrics depend on the size of the crystallites [4], making the preparation of these materials in the form of nanocrystals and nanocomposites of interest. Generally, nanocrystalline materials have large surface-to-volume ratios, and their various properties such as stability, melting temperature, sintering ability, electronic structure, *etc*. depend on the size of the nanocrystallites [5]. Moreover, the second component (matrix, heterogeneous admixture) in nanocomposites can influence significantly the properties of the first (active) component (preferred orientation [6], stability of phases [7], and application properties, *e.g*. ionic conductivity [8]).

The purpose of this paper is the study of the $PbTiO_3$ crystallization in pure nanopowders and $PbTiO_3$–SiO_2 (1:1 v/v) nanocomposite powders prepared by the sol-gel technique. The evolution of nanocrystallite particle size at crystallization was estimated from the X-ray diffraction line profile analysis.

Results and Discussion

Samples of $PbTiO_3$ nanopowders and $PbTiO_3$–SiO_2 (1:1 v/v) nanocomposites were annealed at various temperatures for various times. The X-ray diffraction patterns in Figs. 1 and 2 indicate that the crystallization starts in pure $PbTiO_3$ powders at 400°C and in $PbTiO_3$–SiO_2 nanocomposites at 700°C. The SiO_2 phase remains amorphous even after annealing at 800°C for one hour. Differential scanning calorimetry (DSC) agrees with X-ray diffraction concerning the start of crystallization – the first detectable DSC anomaly at about 490°C indicating the existence of a cubic-to-tetragonal phase transition in $PbTiO_3$ (*i.e*. the presence of a crystalline phase) was found in pure $PbTiO_3$ samples annealed at 500°C and in $PbTiO_3$–SiO_2 samples annealed at 800°C. This is comparable with the crystallization

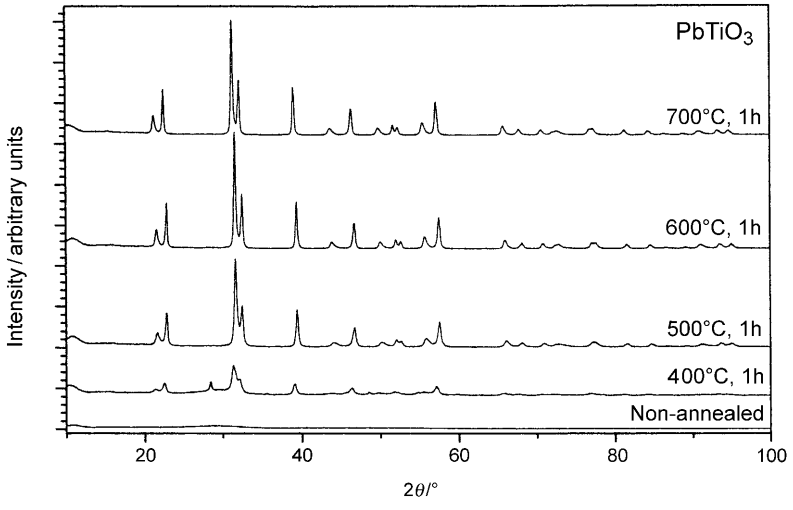

Fig. 1. Powder diffraction patterns of annealed pure $PbTiO_3$ powders

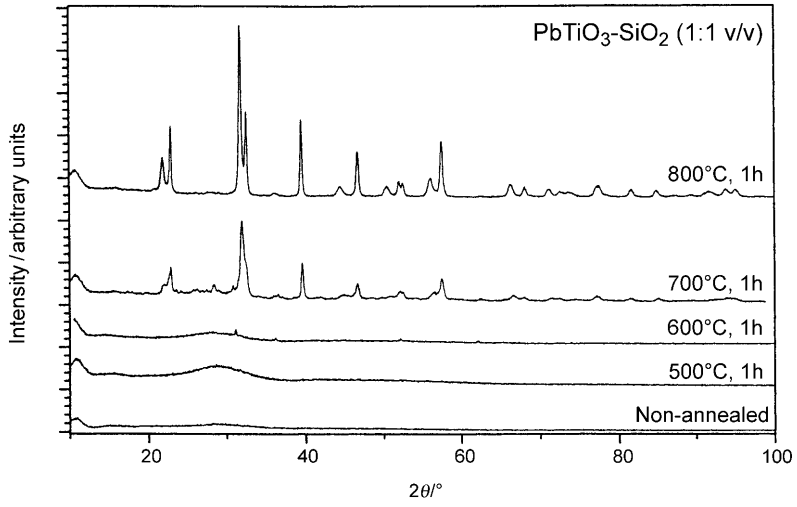

Fig. 2. Powder diffraction patterns of annealed $PbTiO_3$-SiO_2 nanocomposites

temperature (800°C) of $PbTiO_3$ in $PbTiO_3$–SiO_2 glass ceramics with a high content of SiO_2 ($PbTiO_3$:SiO_2 = 8.4:91.6 mol%) prepared by the sol-gel technique [9]. In contrast to amorphous SiO_2 in our nanocomposites, SiO_2 crystallized as cristobalite at 800°C in the glass ceramics mentioned above [9]. The hindering effect of a heterogeneous admixture on $PbTiO_3$ crystallization was also observed in $PbTiO_3$–SiO_2–B_2O_3 glass ceramics prepared by the sol-gel process [10, 11]. The crystallization temperature of $PbTiO_3$ increased with rising content of glassy phase [10, 11]. A similar effect was observed in $PbTiO_3$–Al_2O_3 nanocomposite thin films and, to much less extent, in $PbTiO_3$–Al_2O_3 multilayers [12] where the interface area is much smaller than in nanocomposites. The above data imply that the interface interaction between the components of nanocomposites plays an important role in influencing the crystallization of $PbTiO_3$ (and also SiO_2) phases. This is in agreement with the fact that interface interaction can stabilize an amorphous phase at the interface [7, 8].

In Tables 1 and 2, the parameters of annealing are shown together with the corresponding values of crystallite size D (size of coherently scattering regions) and values of microstrain e for $PbTiO_3$ powders and $PbTiO_3$–SiO_2 nanocomposites. The values of crystallite size taken from Tables 1 and 2 are plotted in Fig. 3. From Tables 1 and 2 and Fig. 3 it can be concluded that the size of nanocrystallites increases at higher temperature and time of annealing, the influence of temperature being more significant than that of the time. This is also illustrated in Fig. 4 for both nanopowder and nanocomposites. It should be stressed that X-ray diffraction line profile analysis estimates the size of coherently scattering regions, *i.e.* the size of (nano)crystallites. Each grain of powder can contain several nanocrystallites.

The values of the microstrain e (Tables 1 and 2) are relatively small compared to the values obtained for other nanostructured materials and other methods of preparation. For example, $e = 0.013$ was found for CuO prepared by ball milling [14], values of 0.002 and 0.010 were determined for nanocrystalline Pd obtained by the gas condensation method [15]. The sol-gel method results in smaller

Table 1. Crystallite size D and microstrain e in $PbTiO_3$

Annealing temperature t/°C	τ/h	D/nm	$e \times 10^4$
400	0.5	26	12.7
400	1	28	10.1
500	0.5	32	5.0
500	1	35	14.9
500	2	39	2.5
500	4	43	4.2
600	0.5	72	3.9
600	1	81	5.1
700	0.5	82	4.6
700	1	108	8.6

Table 2. Crystallite size D and microstrain e in $PbTiO_3$–SiO_2

Annealing temperature t/°C	τ/h	D/nm	$e \times 10^4$
700	0.5	36	9.5
700	1	38	11.3
700	2	40	13.8
700	4	44	11.9
800	1	42	10.8

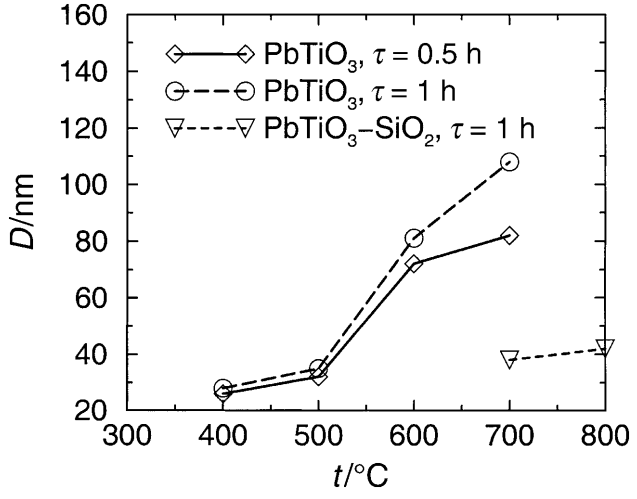

Fig. 3. Dependence of particle size (coherently scattering region) D on the temperature t of annealing at different annealing times τ

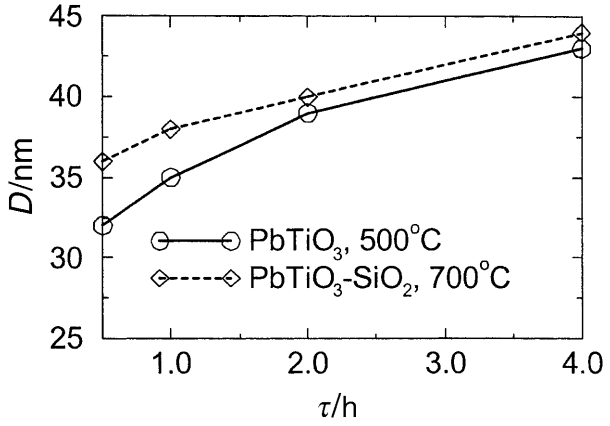

Fig. 4. Dependence of particle size D on annealing time τ

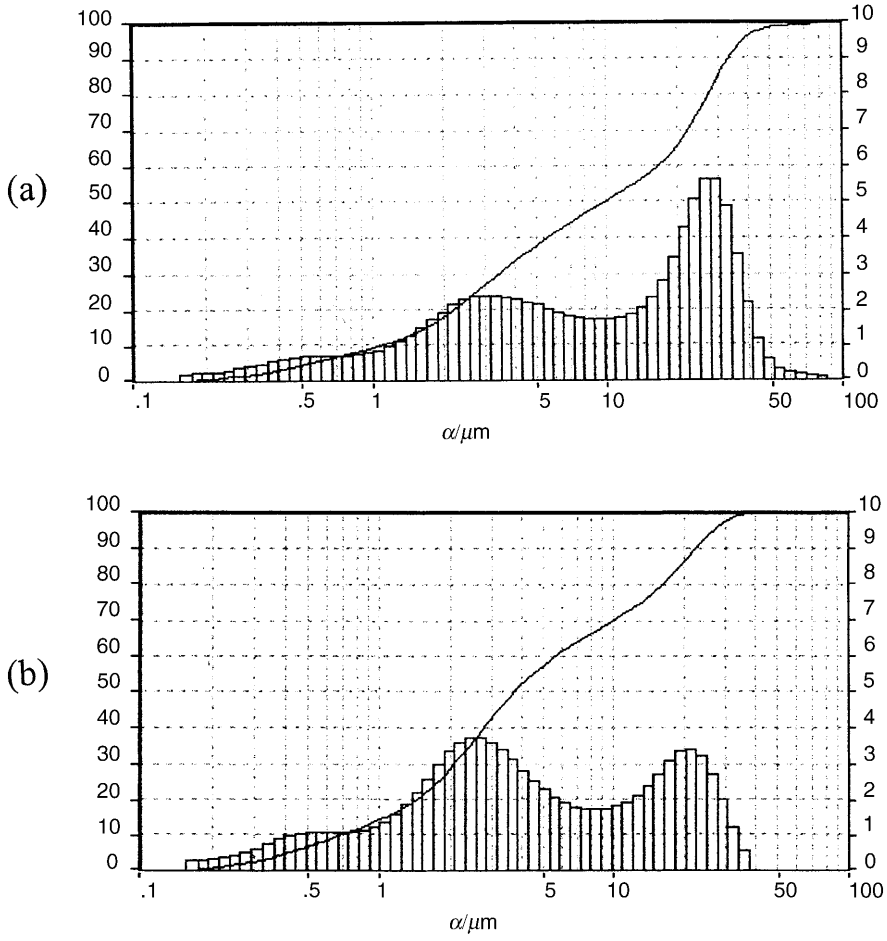

Fig. 5. Results of laser beam scattering experiments; the grain size distribution (relative counts of particles within a given size range) is presented in the form of a histogram (right vertical scale), the integral distribution curve (left vertical scale) is given as a solid line; α: linear grain size; (a) low ultrasound intensity, no detergent used; (b) high ultrasound intensity, detergent used

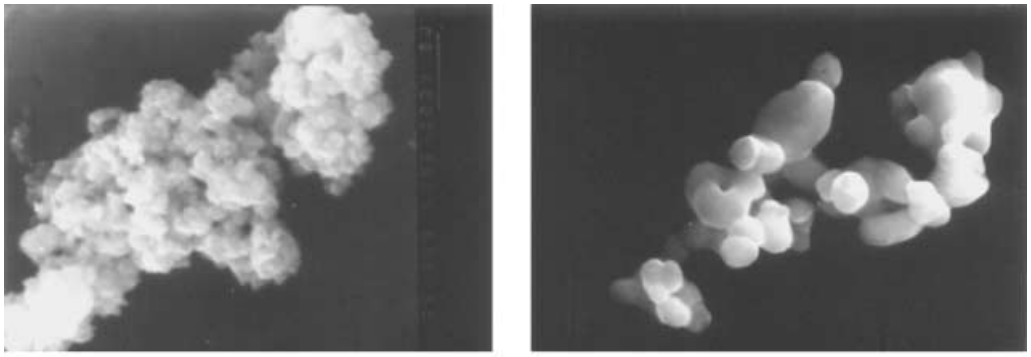

Fig. 6. Scanning electron micrograph of $PbTiO_3$ powder (a) dried for 1 h at 200°C and (b) annealed for 3 h at 800°C; the width of the photograph corresponds to a distance of 4.5 μm

microstrains in nanocrystalline powders than the above mentioned methods. Comparable values of $e = 0.0003–0.0015$ were obtained in nanocrystalline Cu prepared by the electrodeposition technique [16]. Annealing strongly reduces the microstrains in the samples. In our procedure, the ratio of the temperature of annealing (400–800°C) to the melting point of $PbTiO_3$ (1281°C) ranges from 0.43 to 0.69 (for temperatures in K). A significant reduction of microstrains in electrodeposited nanocrystalline Cu was observed for a ratio of 0.31 [16]. However, this ratio approximately equals to 0.69 for cryomilled nanocrystals of Zn [17]. It seems that the effect of annealing on the reduction of microstrains in nanocrystals depends also on the method of preparation. To our knowledge there are no data on microstrains for related materials prepared by the sol-gel method.

Laser beam scattering, which enables to determine the distribution of powder grain sizes (Fig. 5), shows three types of grain sizes: (*i*) agglomerates (10–50 μm) which could be partially destroyed by ultrasound (compare Figs. 5a and 5b), (*ii*) aggregates (1–10 μm) holding together much firmly, and (*iii*) single particles (< 1 μm).

Scanning electron microscopy, which can display the morphology of powder grains, shows a non-annealed $PbTiO_3$ aggregate (in fact, organic compounds are present in it as well) in Fig. 6a and a partially sintered $PbTiO_3$ aggregate after annealing at 800°C for 3 hours in Fig. 6b. The size of the smallest particles forming the aggregate is about 300 nm. As detected by X-ray diffraction, the size of nanocrystallites in this sample is about 159 nm, indicating that the particles can contain a few nanocrystallites in agreement with the results in Ref. [14].

Conclusions

The following conclusions can be drawn from the obtained results:

(*i*) The rate of $PbTiO_3$ crystallization from amorphous powders prepared by the sol-gel technique is stimulated by increased annealing temperatures and to a lower extent, by prolonged annealing time.

(*ii*) The presence of SiO_2 in $PbTiO_3$–SiO_2 (1:1 v/v) composite powders increases the minimum temperature necessary for crystallization by about 300°C in comparison with pure $PbTiO_3$.

(*iii*) Interface interaction between grains of $PbTiO_3$ nanocrystals and an amorphous SiO_2 matrix obviously plays a role in this phenomenon. In order to determine the character of the interaction, further studies have to be performed.

Experimental

$PbTiO_3$ nanopowders and $PbTiO_3$–SiO_2 (1:1 v/v) nanocomposite powders were prepared by the standard sol-gel method [13]. The sol was synthesized by dissolution of water-free lead acetate (trihydrate dried in vacuum at 70°C for 5 h), titanium tetrabutoxide, and silicon tetraethoxide (in the case of the composite) in *n*-butanol. The reaction mixture was stirred and refluxed for 2 h. All operations were performed under dry N_2. The obtained sol was clear and without any solid residues. After cooling to room temperature the sol was rapidly hydrolyzed by a mixture of water and *n*-butanol (1:5 v/v) The resulting white suspension was dried in air at room temperature and then at 140°C (or additionally at 200°C). The obtained white powder was further pulverized in an agate mortar and pressed into a quartz cell for X-ray examination.

X-Ray diffraction measurements were performed with a powder diffractometer using CuK_α radiation from the X-ray source equipped with a rotating anode. The diffractometer was operated with a focusing crystal monochromator in the diffracted beam path and a NaI(Tl) scintillation detector. The fitting procedure of measured diffraction profiles indicated that these profiles could be well approximated by analytical functions of the *Cauchy* type. The same result was obtained for diffraction profiles of the standard sample (tungsten powder). This standard was used to eliminate the instrumental broadening. The *Cauchy* type of measured and standard profiles implies the simple formula $B - b = \beta$ where B, b, and β are the half-widths of the measured profile, the instrumental profile, and the intrinsic (pure) diffraction profile, respectively. An analog linear relation can be assumed for the physical components of the intrinsic diffraction profile. Consequently, the *Williamson-Hall* plot [18] in the linear form $(\beta \cdot \cos\theta)/(K \cdot \lambda) = (1/D) + (4 \cdot e \cdot \sin\theta)/(K \cdot \lambda)$ was used where the half-width of diffraction profile β is given in radians, λ is the wavelength of the X-ray radiation, θ is the *Bragg* angle, D is the crystallite size, $e = \Delta d/d$ is the microstrain (d: interplanar spacing), and K is the *Scherrer* constant depending mainly on the shape of the crystalline particles. Its values are close to 1 [18], and this value was used in our calculations.

The DSC measurements were performed using a Perkin-Elmer DSC7 calorimeter at a scanning rate of 10 K/min. Powder samples (typically 30–40 mg) were placed in sealed aluminum pans, and N_2 (25 cm^3/min) was used as purging gas. Scanning electron microscopy was performed with a JEOL JXA 733 electron microprobe. Laser beam scattering (Fritsch Analysette 22) was used to determine the distribution of powder grain sizes. The powder was dispersed in pure H_2O or in H_2O containing detergent and agitated by ultrasound.

Acknowledgements

This work was supported by the grants IAA1010113, RN 1998 2003 014, NSC 89-211-M-005-022, GA CR 202/96/0425, and GA CR 202/00/1245. We are grateful to *Karel Jurek* for SEM observations, to *Pavel Lejček* and *Vladimír Železný* for fruitful discussions, and to Fritsch company for providing measurement time.

References

[1] Le Marrec F, Fahri R, El Marsi M, Dellis J-L, Ariosa D, Karkut MG (2001) Ferroelectrics **254**: 1
[2] Trainer M (2001) Am J Phys **69**: 966

[3] Auciello O, Scott JF, Rames R (1998) Physics Today, July 22
[4] Tanaka M, Makino Y (1998) Ferroelectric Lett **24**: 13
[5] Wang Z, Saxena SK, Pischedda V, Liermann HP, Zha CS (2001) J Phys Condens Matter **13**: 8317
[6] Buršík J, Vaněk P, Kužel R, Studnička V, Železný V (2001) J Eur Cer Soc **21**: 1503
[7] Uvarov NF, Vaněk P (2000) J Mater Synth Process **8**: 319
[8] Uvarov NF, Vaněk P, Yuzyuk YuI, Železný V, Studnička V, Bokhonov BB, Dulepov VE, Petzelt J (1996) Solid State Ionics **90**: 201
[9] Qi L, Ma J, Cheng H, Zhao Z (1996) J Mater Sci Lett **15**: 1074
[10] Zhai JW, Yao X, Zhang LY (2000) J Electroceramics **5**: 211
[11] Zhai JW, Yao X, Zhang LY (2001) J Inorg Mater **16**: 147
[12] Buršík J, Vaněk P, Studnička V, Ostapchuk T, Buixaderas E, Petzelt J, Krupková R, Březina B, Peřina V (2000) Ferroelectrics **241**: 191
[13] Klein LC (1996) Processing of nanostructured sol-gel materials. In: Edelstein AS, Cammarata RC (eds) Nanomaterials: Synthesis, Properties and Applications. Institute of Physics Publishing, p 145
[14] Stewart SJ, Borzi RA, Punte G, Mercader RC, Garcia FJ (2001) J Phys Condens Matter **13**: 1743
[15] Fitzsimmons MR, Eastman JA, Müller-Stach M, Wallner G (1991) Phys Rev **B44**: 2452
[16] Lu L, Tao NR, Wang LB, Ding BZ, Lu K (2001) J Appl Phys **89**: 6408
[17] Zhang Z, Wang H, Narayan J, Koch CC (2001) Acta Mater **49**: 1319
[18] Klug HP, Alexander L (1974) X-Ray Diffraction Procedures for Polycrystalline and Amorphous Materials, 2nd edn. Wiley, New York

Received October 4, 2001. Accepted (revised) December 14, 2001